Numerical Simulation of the Particle Deposition Characteristics Inside a Scale Hybrid Particulate Collector

Qianlong Li , Shaojie Guo , Zhengwei Long *

Posted Date: 9 May 2024

doi: 10.20944/preprints202405.0533.v1

Keywords: ESP; fabric FILTER; collection efficiency; cake; numerical model

Article

Numerical Simulation of the Particle Deposition Characteristics Inside a Scale Hybrid Particulate Collector

Li Qianlong, Guo Shaojie and Long Zhengwei

School of Environmental Science and Engineering, Tianjin University, 92 Weijin Road, Tianjin, 300072, China
* Correspondence: author's email address: longzw@tju.edu.cn

Abstract: The control of the fine particle emission from the coal-fired power plants has been a big challenge in china. Either the conventional electrostatic precipitator or the fabric filter has some shortages. The electrostatic precipitator is hard to keep high efficiency for the submicron particles. The fabric filter could keep high efficiency but with very high pressure drop. One solution is to combine them together. Several types of hybrid particle collectors (HPC) combining the electrostatic precipitator and the fabric filter together have been developed and applied in a number of projects in China. In recent years, numerical simulation technology has been widely used in the design of the collectors. In this paper, an unsteady numerical model is used to investigate the particle deposition characteristics in a scale hybrid collector. The fluid field is modeled by using incompressible Navier-Stokes equations with the RNG turbulence equations. The corona discharge is solved by using a finite volume method. The particle charging is modeled by using a filed-diffusing combined model. And an unsteady cake formation model is used to simulate the filtration process.

Keywords: ESP; fabric FILTER; collection efficiency; cake; numerical model

1. Introduction

In China's energy structure, the thermal power equipment capacity has risen to 72% of the total installed capacity [1]. These thermal power plants have been generating a lot of air pollution emissions, such as NO_x, SO_2, particulates and heavy metals. The particulates are mostly the inhalable particulate matters (PM_{10}), whose diameters are lower than 10 μm [2]. Inhalable particulate is a major threat problem to human health [3]. The main control technologies used presently in the power plants include the electrostatic precipitator (ESP) and the fabric filter (FF). Both of them have low collection efficiency for the fine particles ($PM_{2.5}$), whose diameters are lower than 2.5 μm [4]. The results of the site tests from several power plants [5,6] show that the collection efficiency of the ESP and the FF is lower than 90% for the particles in the size range from 0.1 to 1 μm. Thus, some new technologies for the fine particle control have been proposed. Among them, the hybrid particulate collector (HPC) which combines the ESP and the FF together is widely used in China [7]. In recent years, numerical simulation technology has been widely used in the design of the collectors [8–11].

The advanced hybrid particulate collector (AHPC) is a new type precipitator [12] (Figure 1). The bags and the ESP are placed in the same housing, working synergically both in the particulate collection and in the dust cleaning. The AHPC provides ultrahigh collection efficiency, overcoming the problem of excessive fine-particle emission with conventional ESPs, and it solves the problem of re-entrainment and re-collection of dust in conventional baghouses. The experimental works show that the AHPC can achieve the particulate collection efficiencies of 99.99% for particle sizes from 0.01 to 50 μm. For economical consideration, the AHPC can work at a much higher air-to-cloth ratio with respect to the conventional fabric filters. The flue gas first flows into the ESP zone to remove the most particles (about 90% by mass), and then goes through the holes in the perforated plates into the fabric filtration zone to remove the left particles. Hence, the pressure drop through the fabric filters can be very low which means that the fabric filters have longer life.

Preprints.org (www.preprints.org) | NOT PEER-REVIEWED | Posted: 9 May 2024 doi:10.20944/preprints202405.0533.v1

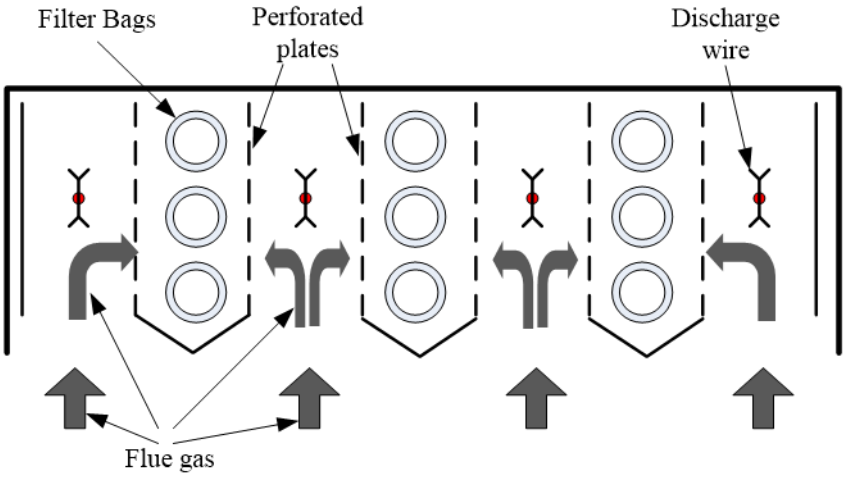

Figure 1. Mechanism description of the hybrid particulate collector.

As the AHPC's structure is very unique, its design needs some new criteria. Experimental work could solve some problems but not totally. Numerical method is a good way, as all the details can be obtained if the model is strong enough. In this work, an unsteady numerical model is used to investigate the particle deposition characteristics in a scale AHPC, which is shown in Figure 2. The scale AHPC includes ten discharge wires, two perforated-plates with twenty-six staggered holes and eight bags (numbered 1 to 8 from left to right). In the simulation, the fluid field is modeled by using the unsteady time-averaged Navier-Stokes equations with the RNG $\kappa-\varepsilon$ turbulent equations. The corona discharge field is analyzed by using a finite volume method. Particle dynamics are modeled by using the Lagrangian method with a field-diffusion combined charging model. For the bag filter, the pressure drop is divided to two parts: the pressure drop across the clean filter and the pressure across the cake on the bag surface. The pressure drop across the cake is related to the mass density of the deposited cake in the surface of bags.

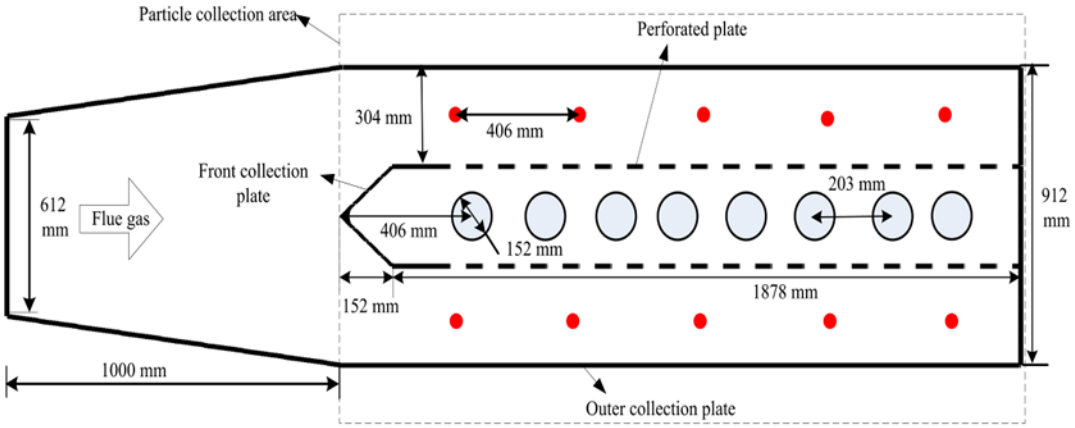

Figure 2. The scale AHPC.

2. Model Description

2.1. Electrostatic Precipitation Model

The physical fields in the AHPC include the fluid flow, the corona discharge, the particle charging, the particle dynamics and the filtration. The coupled effects between the fields should be considered too.

For the corona discharge, the equations can be expressed in dimensionless forms as follow [13]:

 doi:10.20944/preprints202405.0533.v1

$$\nabla^2 V' = -(\frac{\rho_w}{\varepsilon_0 V_w})\rho_s' \tag{1}$$

$$\nabla \bullet \mathrm{J} = 0 \tag{2}$$

$$\mathrm{J} = b_i \mathrm{E} \rho_s' \tag{3}$$

$$\mathrm{E} = -\nabla V' \tag{4}$$

where V is the electric potential (V), V_w the electric potential at the corona wire, $V' = V / V_w$, ρ_w the space charge density at the corona wire (C/m^3), ρ_s the space charge density and $\rho_s' = \rho_s / \rho_w$, ε_0 the air permittivity ($8.85\times10^{-12}\ C^2/N\bullet m^2$), J the current density (A/m^2), b_i the ion mobility ($m^2/V\bullet s$), E the electric field (V/m).

As the pressure drop across the bag filter increase along with the filtration, the fluid flow is unsteady. Besides, the flow field is influenced by the electric field, namely the electro-hydrodynamic (EHD). This paper solves the full Navier-Stokes equations with the RNG turbulent equations [14]:

$$\frac{\partial U_i}{\partial x} = 0 \tag{5}$$

$$\rho_f \frac{\partial U_i}{\partial t} + \rho_f \frac{\partial U_i U_j}{\partial x_j} - (\mu + \mu_t)\frac{\partial}{\partial x_j}(\frac{\partial U_i}{\partial x_j} + \frac{\partial U_j}{\partial x_i}) = -\frac{\partial P}{\partial x_i} + F_{ci} + \rho_f g_i \tag{6}$$

where $U_i (i = 1,\ 2,\ 3)$ is the fluid velocity (m/s), ρ_f is the fluid density (kg/m^3), t is the time (s), μ is the laminar viscosity ($kg/m\bullet s$), μ_t is the turbulent viscosity ($kg/m\bullet s$), P is the fluid pressure (Pa), F_{ci} is the electric body force (N/m^3), g_i is the acceleration of gravity (m/s^2).

The RNG turbulent model is derived from the application of a rigorous statistical technique to the instantaneous Navier-Stokes equations. It is suitable for the problems with high streamline curvatures [15]. An unstructured finite volume method has been developed to solve this equation system [16]. The fluid filed equations are solved by using the CFD package Fluent [17]. The inlet boundary condition is the velocity-inlet and the outlet one is the outflow. The boundary condition of the walls is the wall function. The program for solving the corona discharge equations is linked to the Fluent by using the user defined functions (UDF).

The particle dynamics is modeled by using Lagrangian method [18]. According to the Newton's second law, the equation that describes the particle motion is written as:

$$\frac{d\mathrm{U_p}}{dt} = C_\mathrm{D}\frac{3\rho_f \left|\mathrm{U}-\mathrm{U_p}\right|(\mathrm{U}-\mathrm{U_p})}{4\rho_\mathrm{p} d_\mathrm{p}} + g + \frac{3\mathrm{E}q_\mathrm{p}}{4\rho_\mathrm{p} d_\mathrm{p}^3} \tag{7}$$

where $\mathrm{U_p}$ is the local particle velocity, U is the local fluid velocity, ρ_p is the particle density, d_p is the particle diameter, q_p is the particle charge (C), C_D is the drag force coefficient, g is the gravity gradient.

The drag force coefficient C_D can be expressed as a function of the particle Reynolds number $\mathrm{Re_p}$ as follows:

$$C_\mathrm{D} = a_1 + a_2/\mathrm{Re_p} + a_3/\mathrm{Re_p^2} \tag{8}$$

$$\mathrm{Re_p} = \frac{\rho_f \left|\mathrm{U}-\mathrm{U_P}\right| d_\mathrm{P}}{\mu} \tag{9}$$

 doi:10.20944/preprints202405.0533.v1

The turbulence has strong effect on the particle motion, namely the turbulence dispersion. In the present work, the discrete random walk (DRW) model [19] is used.

The particle charge q_P in the Eq. (7) is calculated by using a field modified diffusion (FMD) model [20]. The charging rate is expressed in the following dimensionless form:

$$\frac{\mathrm{d}v}{\mathrm{d}t_q}=\begin{cases} f(w)\dfrac{v-3w}{\exp(v-3w)-1}, & v>w \\ \dfrac{3w}{4}(1-\dfrac{v}{3w})^2+f(w), & -3w\le v\le 3w \\ -v+f(w)\dfrac{-v-3w}{\exp(-v-3w)-1}, & v<-3w \end{cases} \tag{10}$$

where $f(w)$ is the fraction of the surface covered by the diffusive band:

$$f(w)=\begin{cases} \dfrac{1}{(w+0.475)^{0.575}}, & w\ge 0.525 \\ 1, & w<0.525 \end{cases} \tag{11}$$

where v ($=\dfrac{q_p e}{2\pi\varepsilon_0 d_p kT}$) is the dimensionless particle charge, w ($=\dfrac{K_p}{K_p+2}\dfrac{Ed_p e}{2kT}$) is the dimensionless electric field, and $t_q(=\dfrac{\rho_s b_i t}{\varepsilon_0})$ is the dimensionless particle charging time, k is Boltzmann's constant ($1.38\times10^{-23}\,J/K$), T is the temperature (K), e is the charge on an electron ($1.6\times10^{-19}\,C$), K_p is the particle dielectric constant, E is the local electric field (V/m), ρ_s is the space charge density (C/m^3).

The particle motion equation (7) is solved by using the *Fluent* program and the program for solving the particle charge equations (10)-(11) is linked to the Fluent by using the UDF.

2.2. Filtration Model

In the simulation, the particles will deposit on the bag surface to form a cake. There are two pressure drops: the one across the filter body and the one across the cake (Figure 3):

$$\Delta P=\Delta P_c+\Delta P_f \tag{12}$$

where ΔP is the total pressure drop, ΔP_c the pressure drop across the cake and ΔP_f the pressure drop across the filter.

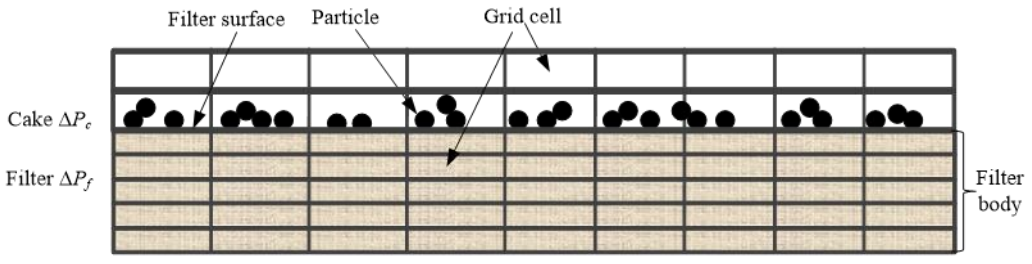

Figure 3. Schematic view of the filtration model.

The pressure drop across the filter body dependents only on the filtration velocity. And the pressure drop across the cake can be related to the filtration velocity according to the Kozeny-Carman equation [21]:

Preprints.org (www.preprints.org) | NOT PEER-REVIEWED | Posted: 9 May 2024 doi:10.20944/preprints202405.0533.v1

$$\Delta P = \frac{180(1-\varepsilon_c)}{\varepsilon_c^3}\frac{1}{\rho_p d_p^2}\mu V_f M_c \tag{13}$$

where ε_c is the cake porosity, ρ_p the particle density, d_P the particle diameter, V_f the filtration velocity, μ the air viscosity and M_c the cake mass density.

The cake porosity ε_c can be related to the particle diameter as [22]:

$$\varepsilon_c = 1-0.58\left[1-\exp(\frac{-d_p}{0.53})\right] \tag{14}$$

Thus, the pressure drop can be written as:

$$\Delta P = \frac{104\left[1-\exp(\frac{-d_p}{0.53})\right]}{(1-0.58\left[1-\exp(\frac{-d_p}{0.53})\right])^3}\frac{1}{\rho_p d_p^2}\mu V_f M_c \tag{15}$$

In the simulation, the bag filter is modeled as a porous media. And the cake mass density is calculated by using the total mass of the particles that reach the bag surface piece.

2.3. Model Validation

The particle collection efficiency data of Kihm (1987) was use to validate the electrostatic precipitation model [23]. The model ESP consists of eight smooth round discharge wires with diameter 100 μm. The seeded droplets has a mass flux of about 7.49e-10 kg/s with uniform diameter 4 μm. The applied voltage is positive and ranged from approximately 6 kV to 14 kV. The gas velocity is 2 m/s. Figure 4 shows the comparison between the model predictions and the experimental data. It proves that the model could be used to prediction the collection efficiency of the electrostatic precipitator.

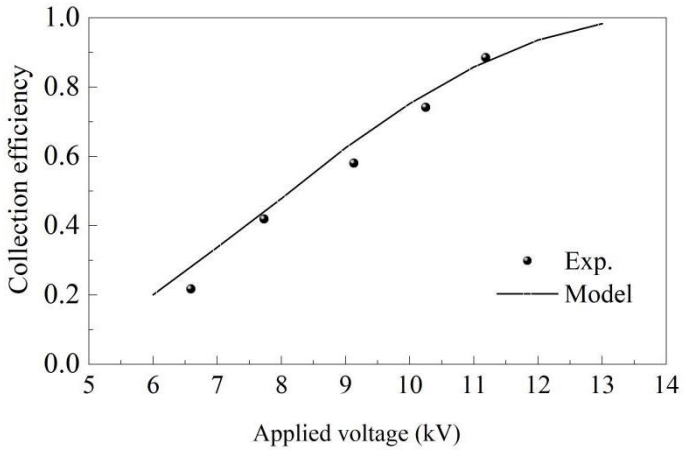

Figure 4. Comparison of the model predictions with the experimental data.

3. Case Setup and Parameters

In the simulation, the mean filtration velocity is set to 3.6 m/min. Thus, the inlet gas velocity equal 0.37 m/s. To consider the turbulent dispersion, the inlet gas is thought to be the full developed turbulence flow. The outlet boundary condition is pressure-outlet.

The scale AHPC has ten discharge wires. The wire diameter is 0.24 mm. The wire-wire space is 406 mm and the wire-plate space is 152 mm. Its current-voltage characteristic is calculated by using the semi-empirical theories, which have the following uniform formula:

 doi:10.20944/preprints202405.0533.v1

$$i_0 = k_v V(V - V_s) \tag{16}$$

where i_0 is the plate current density (mA/m²), V is the applied voltage (V), k_v is the geometry parameter, and V_s is the corona onset voltage (V).

In this paper, the average values of two semi-empirical theories [24,25] are used. The current-voltage characteristic of the scale AHPC is shown in Figure 5.

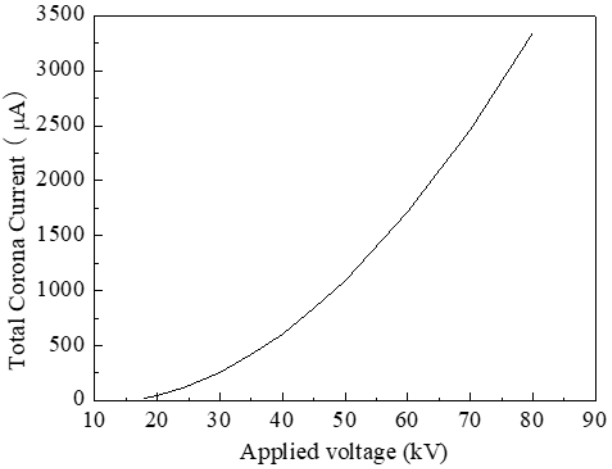

Figure 5. The calculated current-voltage characteristic of the scale AHPC.

This work adopts the mono-disperse fly ash as the seed particle. The particle density is 2600 kg/m³. The particles are injected into the flow from the inlet face with the same velocity as the gas. The particle mass flux is set to 7.7×10^{-4}kg/s. In the simulation, the time step is set to 1 second. The particles are injected into the flow once every second. Every time when the particles are injected, the pressure drops across the filter body and the cake are updated and the flow solver iterates until convergence. The total time of injecting particles is 600 second.

4. Results and Discussion

In the simulation, four types of particle size are considered: 0.1, 0.3, 1 and 3μm. The applied voltage is fixed at 40 kV.

Figure 6 shows the normalized voltage and the charge density distributions. The isolines of the voltage are orthogonal with that of the charge density. The results suggest that the perforated plates have good electric field shielding effects. Both the voltage and the charge density around the bags are very low. The charges are driven to the plates along the electric field lines. It is clear that part of charges reach the sides of the perforated plates facing the bags. Thus, it could be concluded that part of the charged particles will deposit those sides.

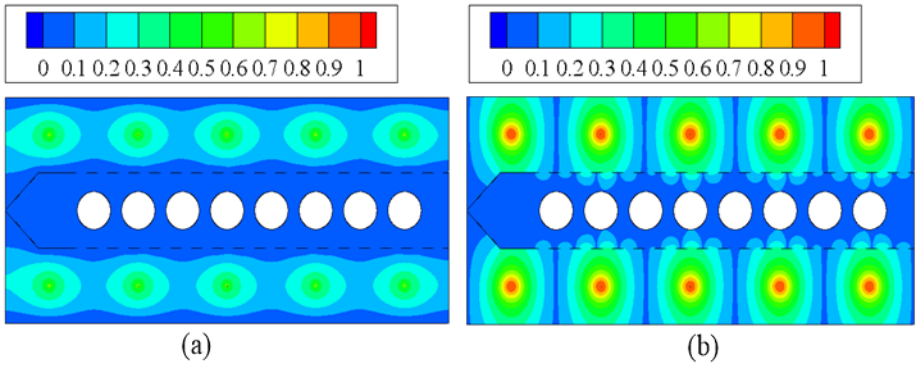

Figure 6. The normalized voltage (a) and charge density (b) distribution of the scale AHPC at 40kV.

 doi:10.20944/preprints202405.0533.v1

Figure 7 shows the stream line distribution in the scale AHPC without the particles. In each bag, one small square is added at the center. These squares are used to be the flow outlets. The gas flows into the electrostatic area firstly and then enters into the filtration area through the holes of the perforated plates. It is clear that the flow is influenced by the electric field. The streamlines have some wrinkles near the discharge wires. In most areas, the flow is irrotational. But in some places there are some vortexes. The first place is at the first hole of the perforated plate. The gas flows past this hole and then forms a vortex. The other places are at the tail area of the AHPC. The vortexes are not good for the collecting particles. The fine particles will follow the streamlines of the vortexes and are hard to deposit. Besides, the vortexes near the collecting plates will make the deposited particles re-entrain.

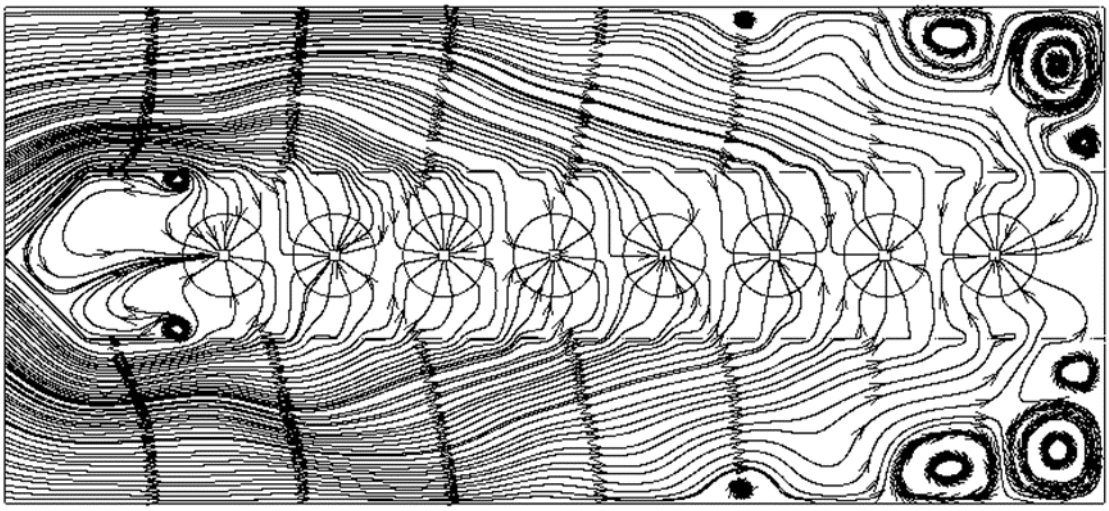

Figure 7. The stream line distribution of the scale AHPC without particles.

Figure 8 presents that the total mass of the deposited particles on the eight bags and the ESP collection efficiency. The results show that the particle mass decreases approximate linearly from the second bag from the left to the right-most bag. But the particle mass on the first two bags from the left are very close. As the eight bags have nearly the same surface filtration velocities, the pressure drops across the bags will be positive related to the deposited particle mass. Thus, higher particle mass results higher pressure drop. The bags with higher deposited particles will be more dangerous to be damaged. It is best to avoid this. One way is to design different hole size for the perforated plate. The hole size should get bigger from the left to the right. This will make more gas flow through the perforated plate from the right bags. The bigger particle size results lower deposited mass. It is also seen from the ESP collection efficiency, which increases approximate linearly with the particle diameter.

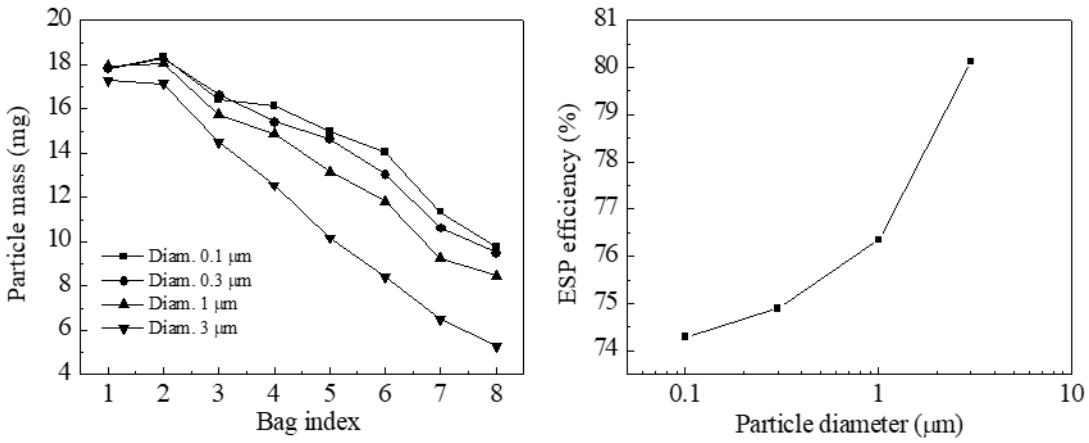

Figure 8. The total particle mass of eight bags and the ESP efficiency for four particle sizes.

 doi:10.20944/preprints202405.0533.v1

5. Conclusion

In this work, a numerical model for simulating the electrostatic fabric filter is presented. And the particle collection characteristics of a scale hybrid particulate collector are investigated. From the results of modeling, the following conclusions can be given:

1: The perforated plates have good electric field shielding effects.

2: Some vortexes exist at the area near the end of the hybrid particulate collector.

3: The particle size has no influence on the flow distribution between the bags. And the mass flow rate across each bag is very uniform.

4: From the first bag at the left to the last bag at the right, the deposited particle mass on the bag surface decreases. And the collection efficiency of the electrostatic zone increases approximate linearly with increasing the particle size.

Acknowledgments: This research has been supported by National Key Research and Development Plan of the Ministry of Science and Technology of China (Grant No. 2022YFB4100702) and National Science Foundation of China (Grant No.51878442).

References

1. China's National statistical bulletin, 2010.
2. Zhang Chengfeng, Yao Qiang, Sun Junming. Characteristics of particulate matter from emissions of four typical coal-fired power plants in China. Fuel Processing Technology, 2005, 86: 757-768.
3. D. W. Dockery, and C. A. Pope. Acute Respiratory Effects of Particulate Air Pollution. Annual Review of Public Health, 1994, 15: 107-132.
4. Hinds W C. Aerosol Technology: Properties, Behavior, and Measurement of Airborne Particles. Wiley, New York, 1999.
5. Yi H, Hao JM, Duan L, et al. Characteristics of inhalable particulate matter concentration and size distribution from power plants in China. J. Air & Waste Manage. Assoc., 2006, 56:1243-1251.
6. Yi H, Hao JM, Duan L, et al. Fine particle and trace element emissions from an anthracite coal-fired power plant equipped with a bag-house in China. Fuel, 2008, 87:2050-2057.
7. HUANG Wei, LIN Hong, ZHENG Kuizhao. The R&D and Application of Electrostatic-Fabric Organic Integrated Precipitator in China. The 11th International Conference on Electrostatic Precipitation, Hangzhou, China, 2008, pp. 464-467.
8. Zhuangbo Feng, Wuxuan Pan, Hao Zhang, Xionglei Cheng, Zhengwei Long, Jinhan Mo. Evaluation of the performance of an electrostatic enhanced air filter (EEAF) by a numerical method. Powder Technology, 2018, 327: 201-214.
9. Zhuangbo Feng, Wuxuan Pan, Yiwen Wang, Zhengwei Long. Modeling filtration performance of pleated fibrous filters by Eulerian-Markov method. Powder Technology, 2018, 340: 502-510.
10. Zhuangbo Feng, Junyan Yang, Jie Zhang. Numerical optimization on newly developed electrostatic enhanced pleated air filters for efficient removal of airborne ultra-fine particles: Towards sustainable urban and built environment. Sustainable Cities and Society, 2020, 54: 102001.
11. Yuan Jiang, Xiaohong Yan. Numerical investigation of the performance of electrostatic precipitators with wet rope array as collection electrodes. Powder Technology, 2020, 366: 337-347.
12. Zhuang, Y, Stanley. J. Miller. Advance Hybrid Particulate Collector final topic report for phase III, 2001.
13. J. R. McDonald, W. B. Smith, H. W. Spencer III, L. E. Sparks, A mathematical model for calculating electrical conditions in wire duct electrostatic precipitation devices, J. Appl. Phys, 48 (1977), 2231-2243.
14. Launder, B. E., Spalding, D. B. The numerical computation of turbulent flows. Computer Method in Applied Mech. and Eng., 1974, 3: 269-289.
15. Long, Z., Yao, Q. Numerical simulation of the flow and the collection mechanism inside a scale hybrid particulate collector. Powder Technology, 2012, 215-216: 26-37.
16. Long Zhengwei, Yao Qiang, Song Qiang, Li Shuiqing. A second-order accurate finite volume method for computation of electrical conditions inside the wire-plate electrostatic precipitator on unstructured meshes. Journal of Electrostatics, 67 (4) 597-604, 2009.
17. Fluent Inc. Fluent 6.0 user guide, 2001.
18. Clayton T. Crowe, Martin Sommerfeld, Yutaka Tsuji. Multiphase flows with droplets and particles. CRC Press, 1998.
19. Morsi, S. A. and Alexander, A. J. An Investigation of Particle Trajectories in Two-Phase Flow Systems. J. Fluid Mech., 1972, 55 (2): 193-208.
20. Lawless, P.A. Particle charging bounds, symmetry relations and an analytic charging rate model for the continuum regime. J. Aerosol Sci., 1996, 27(2), 191–215.

 doi:10.20944/preprints202405.0533.v1

21. Neiva A, Leonardoa J. A procedure for calculating pressure drop during the build-up of dust filter cakes. Chemical Engineering and Processing, 2003, 42(6):495-501.
22. Thomas D, Contal P, et al. Clogging of fibrous filters by solid aerosol particles Experimental and modeling study. Chemical Engineering Science, 2001, 56(11): 3549-3561.
23. Kihm, K. D. (1987). Effects of Nonuniformities on Particle Transport in Electrostatic Precipitators. Ph.D. dissertation, Department of Mechanical Engineering, Stanford University, Stanford, CA.
24. G. Cooperman, A new current-voltage relation for duct precipitators valid for low and high current densities. IEEE Trans. Ind. Appl., IA-17 (1981): 236-239.
25. J. Böhm, Electrostatic Precipitators. Amsterdam: Elsevier Sci. Pub. Company, 1982.